Isotopic study of the Pb-Zn (Cu-Ag) Santa Maria Deposit, Caçapava do Sul Region, Rio Grande do Sul, Brazil

David Ramos Pereira[1*] ⓘ, Moacir José Buenano Macambira[1] ⓘ, Karen Cristina de Jesus Pires[2] ⓘ, Samuel Bouças do Lago[3] ⓘ

Abstract

The Camaquã Mines, in the central-southern region of Rio Grande do Sul State, Brazil, contain the largest deposits of base metals (Camaquã, Cu; Santa Maria, Pb-Zn) in the Camaquã Basin. The host rocks are consisted of sandstones and conglomerates of the Santa Bárbara Group and interbedded volcanic rocks of undefined stratigraphic position. Peperitic features were identified in a mineralized trachytic sill. An age of 565 ± 5 Ma (U-Pb LA-MC-ICP-MS) was obtained for another trachytic rock, which allowed for the identification, for the first time, of the Acampamento Velho Formation in the Camaquã Mines region. Stratigraphic relations demonstrate that both rocks represent this magmatism. Data from Pb isotopes and spatial relationship observed in the field indicate a possible genetic link between Acampamento Velho Formation and Camaquã mineralization. Pb isotopic data also suggest a predominantly older crustal source (1.07 Ga model age) for Pb and possibly for the other metals, with intermediate or mixed origin, suggesting that magmatic-hydrothermal fluids leached the metals from the percolated rocks of the basement.

KEYWORDS: Camaquã Mines; Pb-Zn (Cu-Ag) Santa Maria deposit; Acampamento Velho Formation; geochronology; Pb isotope geochemistry.

INTRODUCTION

Camaquã Mines correspond to the main deposits of base metals of the Camaquã Basin, the Camaquã (Cu, Au-Ag) and Santa Maria (Pb-Zn, Cu-Ag), which are settled in conglomerates and sandstones of the Seival and Rincão dos Mouras formations, that belong to the Santa Bárbara Group (Fambrini 2003). They are located near the city of Caçapava do Sul, in the central-southern region of the state of Rio Grande do Sul, and their ore reserves correspond to *ca.* 30 million tons, with an average content of 1.05% Cu (Camaquã deposit, 24 million tons already mined), and *ca.* 33 million tons with an average content of 1.44% Pb and 1.06% Zn (Santa Maria deposit) (Teixeira *et al.* 1978, Badi 1987).

The Camaquã deposit is constituted by the already exhausted Uruguay (open-pit) and São Luiz (underground) mines. It has been known since 1865, when it was discovered by Englishmen, who were mining gold in the Lavras do Sul region. Mining activities developed intermittently, mainly between 1950 and 1996 (Teixeira *et al.* 1978, Laux and Lindenmayer 2000, Remus *et al.* 2000). In this deposit, the ore consists of Cu and Cu-Fe sulfides (chalcopyrite, bornite, chalcocite, and pyrite) associated with

a gangue of quartz, hematite, chlorite, carbonate, and barite (Teixeira and Gonzalez 1988, Ronchi *et al.* 2000).

The Pb-Zn (Cu-Ag) Santa Maria deposit, located 3 km SW from the Uruguay and São Luiz mines, was discovered in 1978 (Licht 1980). According to Badi and Gonzalez (1988) and Remus *et al.* (2000), the ore is formed by Pb-Zn sulfides (galena and sphalerite) and smaller amounts of Cu-Fe sulfides (pyrite, chalcopyrite, bornite, and chalcocite) in a gangue of chlorite, adularia, carbonate, and baryte.

The Acampamento Velho magmatism corresponds to a bimodal plutonic-volcanic sodic alkaline silica-saturated association that developed in the post-collisional stage of the Brasiliano orogeny (Bitencourt and Nardi 2000, Almeida *et al.* 2002, Wildner *et al.* 2002). It has already been identified in several locations in the Camaquã Basin, including the Ramada (Sommer *et al.* 2005, Matté *et al.* 2016), Taquarembó, and Bom Jardim plateaus (Janikian *et al.* 2012), the Bugio (Almeida *et al.* 2012), Tupanci, and Picados Hills (Sommer *et al.* 2017), and Palma (Vedana *et al.* 2017). However, there is no record so far of its occurrence in the region of the Camaquã Mines.

The genesis of the Camaquã Mines has been the subject of a long scientific debate, and the prevailing idea is that it has an epithermal or distal hydrothermal-magmatic origin (Bettencourt 1972, Beckel 1992, Remus *et al.* 2000, Ronchi *et al.* 2000, Laux *et al.* 2005, Renac *et al.* 2014).

This work presents new petrographic, geochronological and isotopic data about both trachytes interbedded with the rocks of the Santa Bárbara Group and the Pb-Zn mineralization from the Santa Maria deposit. Based on these data, a possible genetic relationship between this magmatism and mineralization is discussed.

[1]Universidade Federal do Pará – Belém (PA), Brazil.
E-mails: david.pereira@ig.ufpa.br, moamac@ufpa.br

[2]Regulatory Policy Management, National Mining Agency – Porto Alegre (RS), Brazil. E-mail: karen.pires@anm.gov.br

[3]Nexa Resources – Caçapava do Sul (RS), Brazil.
E-mail: samuel.lago@nexaresources.com

*Corresponding author.

REGIONAL GEOLOGY

The Camaquã Basin rests discordantly on the igneous and metamorphic terrains of the Sul-Riograndense Shield, which registers collisional and accretionary events of the Paleoproterozoic (Trans-Amazonian; 2.2–1.9 Ga) and Neoproterozoic (Brasiliano; 900–540 Ma), that led to the amalgamation of the southwestern part of the Gondwana (*e.g.*, Babinski et al. 1996). The evolution of the Brasiliano orogeny in the southern region of Brazil resulted in a collision between the Rio de La Plata (western) and Kalahari (eastern) cratons, which led to the formation of the Dom Feliciano Belt (Fernandes *et al.* 1992).

Post-collisional magmatism, whose composition varies from shoshonite (Shoshonite Association of Lavras do Sul) to silica-saturated sodic-alkaline (Acampamento Velho magmatism) would have developed between 650 and 560 Ma, associated with mega shear zones (Bitencourt and Nardi 2000, Wildner *et al.* 2002).

Camaquã Basin thickness exceeds 6,000 m and the contacts between its units are defined by angular or erosive disconformities resulting from several episodes of tectonic subsidence (Janikian *et al.* 2003, Fambrini *et al.* 2005). It is filled by the sedimentary and volcano-sedimentary succession of the Camaquã Supergroup (Ediacaran-Eopaleozoic), which was defined by Fragoso-Cesar *et al.* (2003). The basin was subdivided as follows, from base to top: the Maricá Group, Bom Jardim Group, Acampamento Velho Formation, Santa Bárbara Group and Guaritas Group (Fig. 1).

Maricá Group, the Camaquã Basin basal unit, corresponds to a more than 4,000-m-thick volcano-sedimentary succession formed by conglomeratic sandstones, siltites, shales, and sandstones (Paim *et al.* 2000, Borba *et al.* 2006). It represents braided rivers and shallow marine deposits. Its maximum depositional age is 601 ± 13 Ma (U-Pb zircon method; Almeida *et al.* 2012).

Bom Jardim Group consists of a volcanic (andesites), pyroclastic and sedimentary rocks succession with estimated thickness of 4,000 m (Janikian *et al.* 2003). It represents, essentially, delta depositional systems. The Shoshonite Association of Lavras do Sul, part of this group, is composed by Hilario Formation volcanic rocks and by Lavras Granite Complex central portion granitoids (Nardi and Lima 1985). An age of 594 ± 4 Ma (U-Pb zircon method) was obtained for the Lavras Granite (Remus *et al.* 2000).
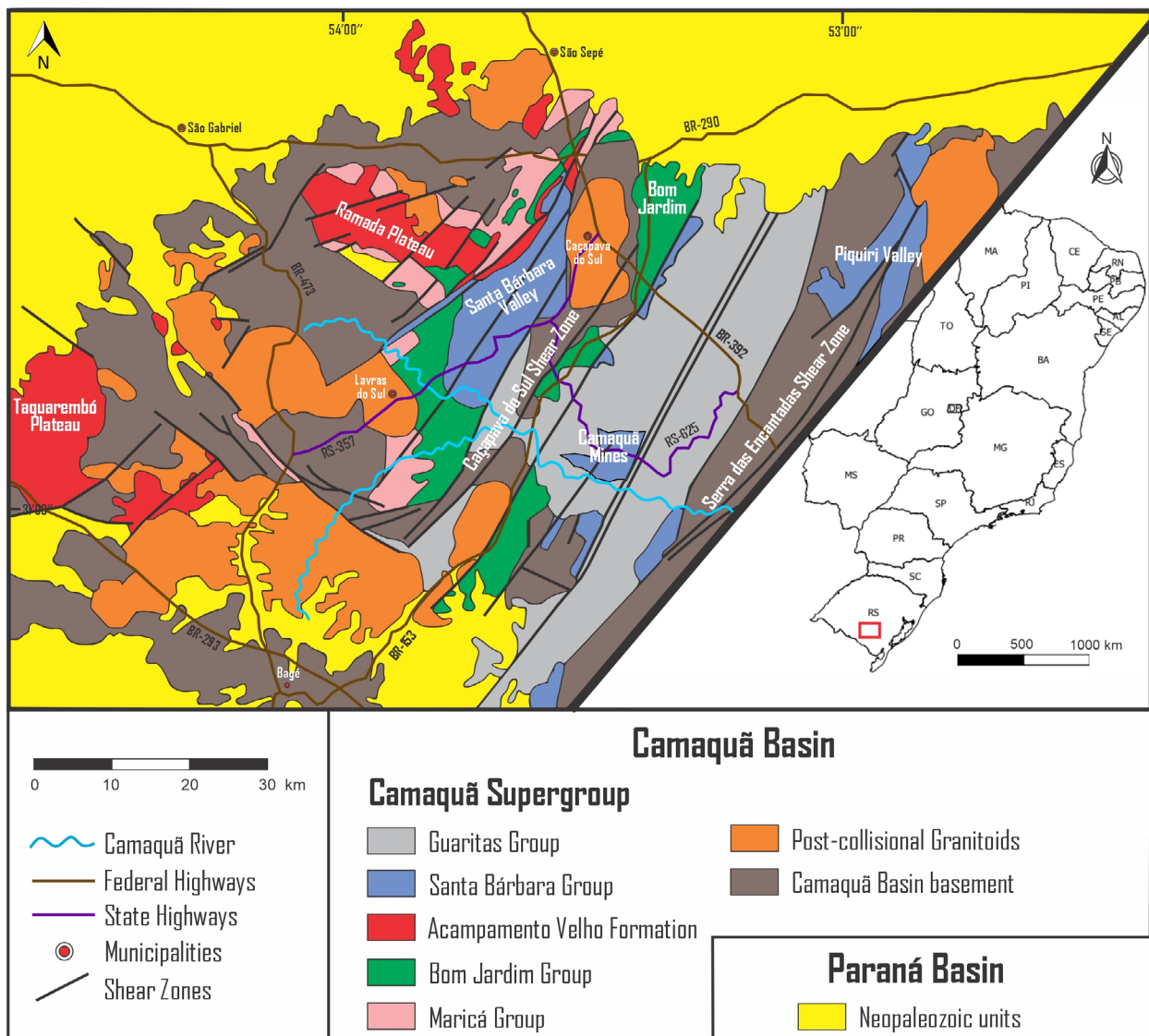
Source: modified from Fragoso-Cesar *et al.* (2000) and Almeida (2005).
Figure 1. Geologic map of the Camaquã Basin and its basement.

Acampamento Velho Formation represents a bimodal volcanic unit of approximately 1,300 m thick, with lower mafic (andesites and basalts) and upper acid successions (tuffs and rhyolites) (Wildner *et al.* 2002). Its age varies between 549 ± 5 and 579 ± 6 Ma (U-Pb zircon; Sommer *et al.* 2005, 2017).

Santa Bárbara Group is formed by sandstones, siltites, and conglomerates that point out alluvial, coastal, and deltaic environments (Fambrini 2003). Its maximum depositional age is 566 ± 7 Ma (U-Pb zircon; Bicca *et al.* 2013).

Guaritas Group, the top unit of the Camaquã Basin, consists of an 800-m-thick succession of sandstones, mainly conglomerates, mudstones, and volcanic rocks (Rodeio Velho member), which were formed in a semi-arid continental environment (De Ros *et al.* 1994, Paim *et al.* 2000). Rodeio Velho andesite rocks were dated at 547 ± 6 Ma (U-Pb zircon; Almeida *et al.* 2012).

Different proposals have been presented for the formation and evolution of this basin (Brito Neves and Cordani 1991, Fernandes *et al.* 1992, Fragoso-Cesar *et al.* 2000, 2003). The dominant interpretation, however, is that a retroarc basin, related to the late to post-orogenic stages of the Brasiliano cycle, evolved into a rift basin in its final stages (Gresse *et al.* 1996, Paim *et al.* 2000, Almeida *et al.* 2012, Oliveira *et al.* 2014).

GEOLOGY OF CAMAQUÃ MINES

The Santa Bárbara Group (Fambrini 2003), which is correlated to the Arroio dos Nobres Formation (Ribeiro *et al.* 1966), encloses most of the sedimentary rocks in the region of the Camaquã Mines. According to Teixeira *et al.* (1978), the magmatism observed in this area corresponds to amygdaloid andesitic volcanic rocks of a brown color, which occur as intercalations or are associated with a regional fault set in the NE direction, and diabase dikes of the Serra Geral Formation, along the NW direction.

Teixeira *et al.* (1978) subdivided the Vargas Member of the Arroio dos Nobres Formation in the region of the Camaquã Mines into the following five lithostratigraphic units: Lower Sandstone, Lower Conglomerate, Middle Sandstone, Upper Conglomerate and Upper Sandstone. Fambrini *et al.* (2005) applied the stratigraphic redefinition of the Santa Bárbara Group proposed by Fambrini (2003) to this region and identified the following formations (from base to top): Passo da Capela, Seival, Rincão dos Mouras and João Dias. A combination of these two stratigraphic classifications is presented on the geologic map of Figure 2.

The Camaquã deposit consists of massive veins, stockworks, and disseminated ore containing Cu and Cu-Fe sulfides (chalcopyrite, bornite, chalcocite, and pyrite) associated with gangue composed mainly of quartz, hematite, chlorite, carbonate, and baryte; traces of Au and Ag are found in the crystalline structure of the sulfides (Teixeira and Gonzalez 1988, Ronchi *et al.* 2000). The Santa Maria deposit (Pb-Zn, Cu-Ag) comprises three mineralized areas (Fig. 2), which contain disseminations, veins, veinlets and stringers, as well as localized massive ore composed of galena and sphalerite, with lower amounts of pyrite, chalcopyrite, bornite, chalcocite, and native copper and silver.

Gangue minerals are chlorite, adularia, carbonate, and baryte (Badi and Gonzalez 1988, Remus *et al.* 2000).

According to Laux and Lindenmayer (2000), the hydrothermal alteration observed in the Uruguay and São Luiz mines is subordinate, being limited in extension to only a few meters from the veins with which it is associated. The hydrothermal minerals are product of chloritization, silicification, and sericitization processes, as well as argilization and sulphidation. The characteristic alteration processes of the Santa Maria deposit correspond to chloritization, sericitization, carbonation, and feldspatization (Remus *et al.* 2000).

METHODOLOGY

In this study, drill core and outcrop samples (provided by the Nexa Resources Company) were obtained from trachytes and host rocks of the mineralization, as well as from country rocks that occur in the region of Camaquã Mines. Polished thin sections were made and described by transmitted and reflected light microscopy at the Institute of Geosciences, *Universidade Federal do Pará* (IG-UFPA). A Scanning Electron Microscope (SEM) (ZEISS, LEO 1430 model) coupled to an Energy Dispersive X-Ray Spectrometer (EDS) (Sirus SD) of the Microanalysis Laboratory, IG-UFPA, and a SEM ZEISS EVO LS 15 coupled to a EDS X-Act SDD 10 mm^2 (Oxford), from the Superintendence of Belém of the Brazilian Geology Survey (*Companhia de Pesquisa de Recursos Minerais* – CPRM), were used to complement the petrographic and minerographic descriptions. Additionally, some of these thin sections were subjected to the double staining process (alizarin + potassium ferrocyanide in diluted HCl) to identify the different carbonate phases.

Analyses by X-ray powder diffraction (XRD) were performed using the X'Pert MPD-PRO PANalytical instrument, which is equipped with a Co anode ($\lambda = 1.7903$), of the X-ray Laboratory, IG-UFPA, at intervals from 4° to 74° (2θ) in total powder, using 5 to 10 g of previously pulverized aliquots. The results were processed using the Match! software and the search for reference standards was performed in the Crystallography Open Database (COD).

The experimental procedure for the Pb analysis in sphalerite followed the techniques developed by Manhès (1982). The leaching techniques were adapted to the conditions of the Pará-Iso Isotopic Geology Laboratory, IG-UFPA, and are described in detail in Galarza and Macambira (2002). However, in this study, the chromatographic separation of Pb was performed with ion exchange resin (Eichrom® Sr 50–100 μm) conditioned with HCl (2N).

Less than 0.5 mg of galena was used in the total dissolution procedure, with a chemical attack made with HBr (8N) + HNO_3 (13N) + H_3PO_4. Then, the sample residue was deposited in a simple rhenium filament for analysis. In both cases of Pb analysis, the final concentrate was analyzed in a thermal ionization mass spectrometer (TIMS) (Thermo-Fischer, Triton Plus model) at the Pará-Iso Laboratory, IG-UFPA. The Pb model age was obtained by averaging the galena compositions and the less radiogenic sphalerite leachates, adopting a

value of μ = 9.74. Regression, age calculations, and isotopic data presented on Pb-Pb diagrams were performed using the Isoplot v.3.68 (Ludwig 2008).

The U-Pb method through LA-MC-ICP-MS in zircon was used to determine the age of crystallization of the trachyte rock. After the experimental procedure for crystal separation, polished sections were prepared, and cathodoluminescence (Mono-CL) images were obtained at the Microanalysis Laboratory, IG-UFPA. In the final stage, these sections were taken to the Pará-Iso Laboratory and analyzed, along with the GJ-1 standard, in the MC-ICP-MS Neptune (Thermo Finnigan) coupled with a Nd:YAG LSX-213 G2 CETAC laser

microprobe. The cup configuration, arranged to simultaneously measure U, Th, Pb, and Hg, was the following: M3 = ^{202}Hg, M4 = ^{204}(Hg+Pb), L4 = ^{206}Pb, M6 = ^{207}Pb, L3 = ^{208}Pb, H2 = ^{232}Th, and H4 = ^{238}U. The Inductively Coupled Plasma (ICP) configurations were: radio frequency power = 1,200–1,300 W; cool gas flow rate = 16 L/min (Ar); auxiliary gas flow rate = 0.7–1.0 L/min (Ar); sample gas flow rate = 1.0–1.3 L/min. The laser setup was: energy = 4–5 J/cm^2, frequency = 10 Hz, spot size = 25 μm, and helium gas flow = 450–500 mL/min. For the calculations of the isotopic ratios (^{206}Pb/^{238}U, ^{207}Pb/^{235}U, and ^{207}Pb/^{206}Pb) and consequently of the ages, the values were corrected from background and ^{204}Hg interference on the ^{204}Pb.
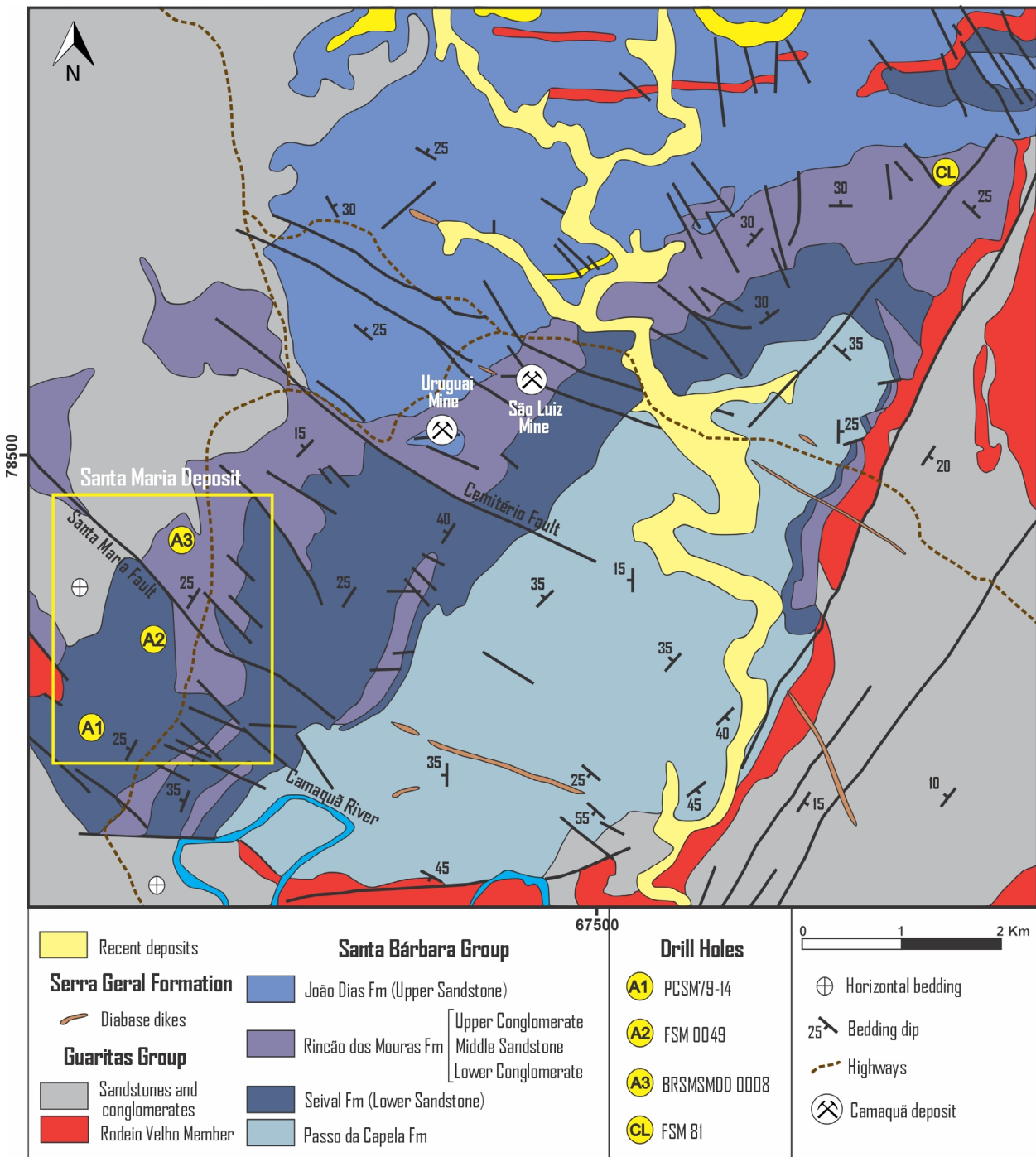
Source: modified from Badi and Gonzalez (1988) and Remus *et al.* (2011).

Figure 2. Geologic map of the Camaquã Mines region with localization of the drill holes selected for the study. The symbology used for representing the drill holes refers to the region in which the samples were collected, as follows: A1 (Area 1), A2 (Area 2), A3 (Area 3), and CL (Claudino farm). CL also represents outcrop samples.

For the correction of common lead contribution, the Stacey and Kramers (1975) terrestrial Pb evolution model has been used. Regression, age calculations, and data presentation in the Concordia diagram were made with Isoplot (v.3.68). A detailed description of the experimental protocol of the U-Pb methodology in zircon by LA-MC-ICP-MS at the Pará-Iso Laboratory can be found in Milhomem Neto and Lafon (2019).

PETROGRAPHY

Four drill holes and one outcrop were selected (Fig. 2) for the study of the trachytic rocks, mineralization, and its country rocks.

Seival Formation

The Seival Formation is predominantly formed by fine to medium-grained sandstones classified as arkoses, which can present rhythmic intercalation with coarse siltstones of similar mineral composition, and more rarely argillites, in addition to subordinate conglomeratic sandstones.

These rocks are red, orange, or white, and have local brecciation, with a moderate to intense degree of oxidation in non-mineralized areas. Sandstones and siltstones are well selected, with flat stratification/lamination and more rarely tabular cross-stratification (in some cases with clay films in the foresets). They consist of angular to rounded grains of quartz, orthoclase, microcline and muscovite, and fragments of volcanic, granitic, schist, sandstone, slate or shale rocks. Biotite, zircon, rutile, magnetite, and apatite occur as trace minerals. Porosity is low (1%) to absent, and both intergranular space and fractures are filled with carbonate and/or illite, which partially replace quartz, muscovite and rock fragments, and more intensely replace orthoclase and microcline. Illite partially replaces carbonate, and both occur in mineralized and altered zones.

Rincão dos Mouras Formation

The Rincão dos Mouras Formation consists primarily of reddish to whitish polymictic conglomerates with sub-rounded to sub-angular pebbles to boulders of gneiss, granitoid, mafic volcanic, sandstone, quartz, and potassium feldspar composition. Locally, interbedded with the conglomerates are levels of coarse to conglomeratic laminated sandstone, dark red laminated siltstone or argillite.

This unit presents inverse gradation (characterized by the predominance of conglomerate at the top and feldspathic conglomeratic sandstone at the base), localized fracturing, and occurs in the upper part of the Area 3 drill hole (BRSMSMDD 0008), reaching a maximum depth of 60 m. The degree of oxidation in this unit is lower than that observed in the Seival Formation. Rutile, zircon, and muscovite are accessory minerals, while carbonate and/or illite fill the intergranular spaces and fractures, and replace the rock grains, as in the Seival Formation.

Acampamento Velho Formation

In the study samples, the Acampamento Velho Formation is represented by two trachytic rocks that occur interbedded with sedimentary rocks, with one in the Seival Formation and the other in the Rincão dos Mouras Formation. The drill holes and outcrop samples selected for this study (Fig. 2) represent such occurrences. One of these drill holes (PCSM79-14) is in Area 1 of the Santa Maria deposit, about 5 km SW of the Camaquã deposit, and another is in the Claudino farm (drill hole FSM 81), about 4 km NE of the Camaquã deposit, where trachyte outcrop samples were also collected.

The trachyte observed in the Seival Formation occurs along about 3.5 m of the PCSM79-14 drill hole from an approximate depth of 131 m. It corresponds to orange to brownish rocks with fine granulation composed essentially of prismatic to tabular crystals of K-feldspar (orthoclase dominantly; minor sanidine) and plagioclase (subordinately) of variable size (0.1–0.4 mm) immersed in brown volcanic glass with variable shades and K-feldspar microliths. It is also characterized by the presence of vesicles, veinlets, and an intense degree of alteration. Iron-magnesium minerals (pyroxene and amphibole) have been entirely replaced. Rutile and apatite crystals have a widespread occurrence.

The observed alterations correspond to ilitization, oxidation, and chloritization, which are associated with the color variation of the rock from orange (when ilitization is predominant) to brown (when oxidation and chloritization prevail).

The vesicles (submillimetric to centimetric) are rounded or elongated, oriented, and filled by gangue minerals of illite, ankerite, siderite, quartz, chalcedony, iron-aluminum-celadonite, and ore minerals of galena, sphalerite, and chalcocite. The veinlets (submillimetric to centimetric) are composed of the same minerals, with a predominance of galena. The vesicles are larger and more frequent at the base, where quartz and chalcedony are predominant, while the top is mineralized and has more veinlets.

The following features of interaction between magma and wet sediment were identified on trachytic rock upper contact (Fig. 3):
- mainly elongated igneous clasts (of millimeter to centimeter size) with edges ranging from rounded, predominantly, to angular, immersed in inequigranular sand matrix (Figs. 3A, 3B and 3C);
- vesicle in igneous clast filled with sediment (Fig. 3A);
- sedimentary clast incorporated in trachyte (Fig. 3B);
- lobe that extends from igneous rock into host sediment (Fig. 3D).

The igneous clasts are concentrated in a thick zone of *ca.* 1 cm parallel to trachytic contact, but also occur scattered upward up to some centimeters (Fig. 3C). The association of these features did allow the characterization of a fluidal or globular peperite (Busby-Spera and White 1987, Skilling *et al.* 2002, Martin and Németh 2007) on top contact of a sill (Allen 1992).

The origin of such peperite is probably related to a sediment fluidization process promoted by intense pore water heating due to magmatic activity, which would have caused the mixing of sediment and subvolcanic clasts (Busby-Spera and White 1987, Skilling *et al.* 2002, Martin and Németh 2007).

Samples of the trachyte that occur in association with the Rincão dos Mouras Formation were collected both at outcrop and drill hole (Fig. 2; FSM 81; about 20 m depth). They correspond to a porphyritic, intersertal, vesicular/amygdaloidal, slightly fractured and very altered rock with a dark gray color, whose porphyries are subhedral columnar crystals of K-feldspar (orthoclase and sanidine; minor plagioclase) with a size varying between 0.7 and 1.2 mm. The matrix consists primarily of K-feldspar laths with a small quantity of volcanic glass between them, in addition to rutile, zircon, and skeletal ilmenite, which occur as accessory minerals. Iron-magnesium minerals (pyroxene and amphibole) have been entirely replaced in this case too. Chalcopyrite occurs as disseminated crystals throughout the rock.

The vesicles are millimetric and filled with aggregates of tiny crystals of quartz, radiating fibrous zeolite crystals, hematite, carbonate (calcite, ankerite and siderite), and chlorite (chamoisite). Quartz and hematite form millimetric to centimetric veinlets.

K-feldspar (and possibly plagioclase) is intensely albitized, being replaced still by calcite, siderite, ankerite, chamoisite, and hematite. Volcanic glass is also chloritized and carbonated and has an intense degree of oxidation (hematite and ulvospinel).

The hematization intensity decreases with depth. In regions close to the surface, transformed considerably to hematite, K-feldspar is more carbonated (calcite), all vesicles are filled and zeolites are more developed. Additionally, quartz is only observed in the vesicles in these regions, filling the largest ones.
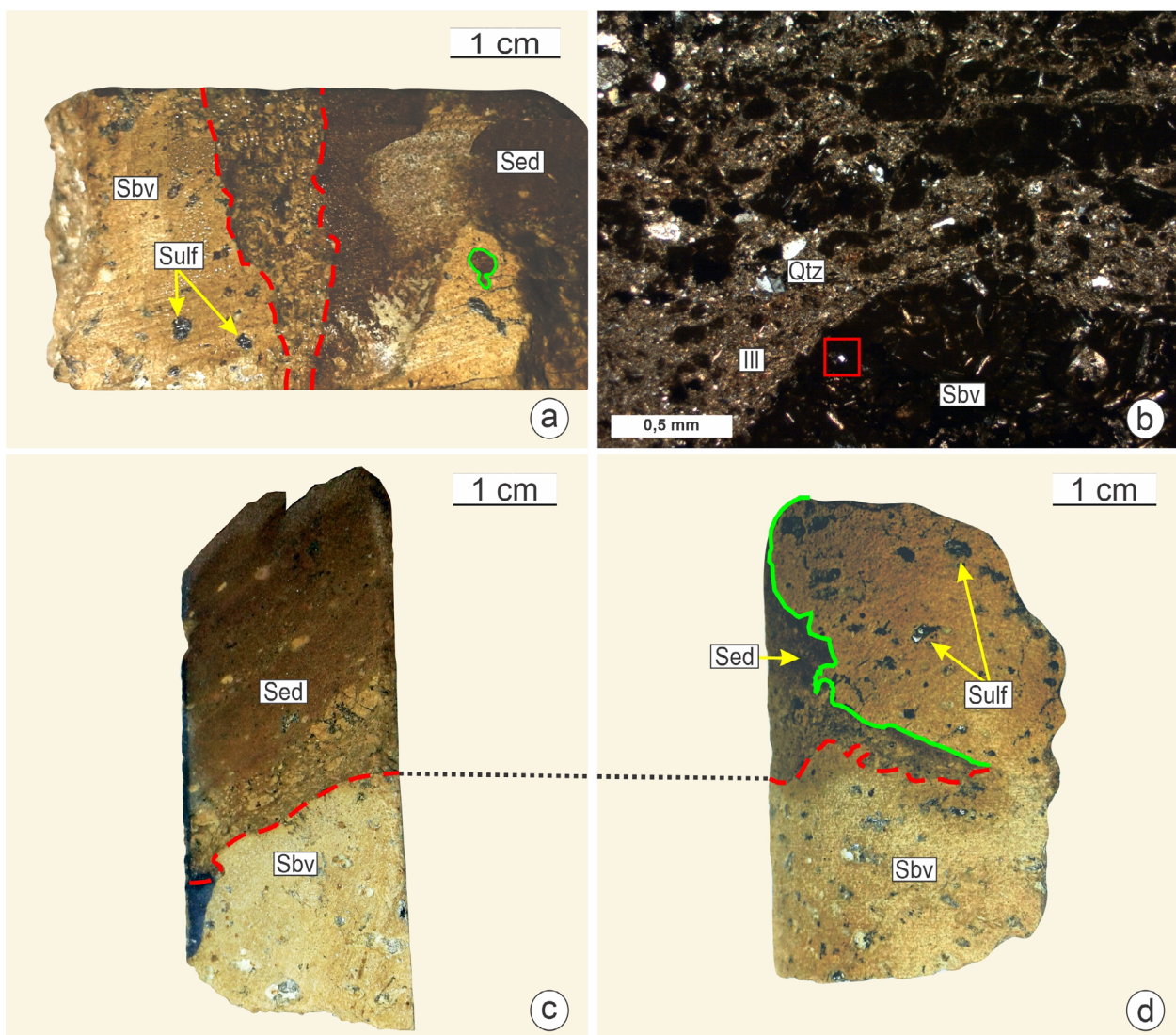
Sulf: sulfide; Sbv: subvolcanic rock; Sed: sedimentary rock; Ill: illite; Qtz: quartz.

Figure 3. Magma-sediment interaction features observed on the top contact of a trachytic (subvolcanic) sill with a sandstone along the PCSM79-14 drill hole; (A) millimetric igneous clasts concentrated at trachyte contact zone (highlighted by red dashed lines); at the inferior right side, a centimetric clast can be observed, in which there is a vesicle filled with sediment (highlighted by green filled line); (B) millimetric igneous clasts commonly elongated with rounded to angular borders and immersed in the sedimentary matrix (transmitted light microscopy, n//); a sedimentary quartz clast assimilated by subvolcanic rock can be observed near the center (highlighted through red square); (C) igneous clasts concentrate just above contact, but also occur dispersed higher up; subvolcanic-sedimentary contact highlighted in red dashed line; (D) subvolcanic lobe (partially delimited in green filled line) that intruded into the sedimentary matrix; subvolcanic-sedimentary contact highlighted in red dashed line; (C and D) represent the same contact (highlighted by black dotted line); therefore, the break in contact continuity in (D) reveals the intrusion of the trachytic lobe into the sedimentary rock.

It was not possible to observe the contact relations of this rock, which hampered the characterization of its placement process. However, field and stratigraphic relations attest to its concordant feature, suggesting it is a sill or a lava flow.

Santa Maria mineralization

Santa Maria ore occurs in all stratigraphic units described so far. The Seival Formation is the main host of the Pb-Zn (Cu-Ag) sulfides (Fig. 2). Galena and sphalerite predominate in relation to pyrite, chalcopyrite, bornite, chalcocite, and native copper and silver. Galena occurs disseminated among rock grains and in K-feldspar cavities, or as massive veins filling fractures/breccias, in which can replace ferroan carbonates. In the Rincão dos Mouras Formation, the Pb-Zn ore consists mainly of galena, sphalerite, and pyrite. Galena presents a similar mode of occurrence to the one of Seival Formation. Sphalerite occurs disseminated and can present intergrowth with galena. In the Area 1 trachytic rock (Acampamento Velho Formation), galena is also the dominant ore mineral, occurring in the vesicles and veinlets. It can present intergrowth with sphalerite, chalcocite, and bornite. Covelite replaces partially to chalcocite. Chalcopyrite and pyrite are disseminated. Claudino farm trachyte, on the other hand, is a barren rock, containing only chalcopyrite as disseminated crystals.

U-Pb GEOCRONOLOGY IN ZIRCON

The crystallization age of the trachytic rock that is interbedded with the rocks of the Rincão dos Mouras Formation was determined by the U-Pb method by LA-MC-ICP-MS using the DMK-CL sample (which includes samples from drill core and outcrop). The analyzed zircon crystals can be morphologically classified into two groups (Fig. 4):

- short prismatic crystals (3:2 length/width ratio; 150 μm in length) and prismatic crystals (2:1 length/width ratio; 200 μm in length), with oscillatory zoning; the core can be homogeneous in some cases (Figs. 4A, 4B, 4C and 4D);
- elongated prismatic (3:1 length/width ratio; 200 μm in length) or elongated crystals (4:1 length/width ratio; 200 μm in length) with only rims partially zoned and a complex (Fig. 4E) or homogeneous (Fig. 4F) core.

Fractures and inclusions are rare. The Th/U ratios between 0.66 and 1.33 of these crystals, their characteristic oscillatory zoning (in most cases) and their dominantly prismatic feature, attest of their magmatic origin (Corfu *et al.* 2003, Xiang *et al.* 2011). Thirty-one analytical points were performed for 30 crystals (Tab. 1; three were discarded for having a high common Pb content) with a variable size of 75–200 μm. Based on the results, the crystals were grouped into three distinct age sets (Fig. 5). The oldest crystals were from Paleoproterozoic, including a grain with 2,357 ± 25 Ma and two grains with a concordant age of 2,035 ± 25 Ma (MSWD = 0.57). One grain presented a Mesoproterozoic age of 1,149 ± 36 Ma. The majority of crystals (n = 17) were from the Neoproterozoic, with ages ranging from 838 to 540 Ma. Within this group, the following concordant ages were obtained: 768 ± 15 Ma (MSWD =

0.43; two crystals), 675 ± 10 Ma (MSWD = 0.30; three crystals), 625 ± 9 Ma (MSWD = 0.45; three crystals), and 565 ± 5 Ma (MSWD = 0.037; nine crystals). There were also seven crystals represented by discordant points, possibly owing to the loss of radiogenic Pb.

The lowest concordant Neoproterozoic age (565 ± 5 Ma) is considered to be the trachyte crystallization age (Fig. 6), while older crystals are interpreted as xenocrystals inherited from basement or sedimentary country rocks. The crystals that define the age of the dated rock have morphological characteristics typical of group 1, dominantly. The inherited zircon crystals have a more variable morphology and can be classified into any of the two groups.

Similar ages to the one obtained for the analyzed trachyte rock, attributed to the Acampamento Velho Formation, characterize the magmatism of several locations in the Camaquã Basin (Tab. 2). However, there are no similar records for the region of the Camaquã Mines. Therefore, this study is the first to present the record of the Acampamento Velho Formation in this region.

Pb ISOTOPIC COMPOSITION OF SULFIDES

Galena samples from the three mineralized areas (one per area) and two sphalerite samples from Area 3 of the Santa Maria deposit were analyzed and plotted on a Pb isotope diagram (Fig. 7; Tab. 3). The galena samples were treated by the total dissolution method, while the sphalerite samples were treated by sequential leaching.

Galena has isotopic ratio values of $^{206}Pb/^{204}Pb$ (16.905–16.983) and $^{207}Pb/^{204}Pb$ (15.487–15.502), similar to those obtained for the first five leached products of the two analyzed sphalerite samples (16.945–16.973 and 15.493–15.528, respectively). Only the final sphalerite residues submitted to total dissolution (L6 of both samples) showed significantly more radiogenic (17.555–17.595 for $^{206}Pb/^{204}Pb$ and 15.552–15.574 for $^{207}Pb/^{204}Pb$).

The isotopic composition of Pb obtained by averaging the galena compositions and the lowest isotopic ratios of sphalerite leachates indicate a primitive source for the Santa Maria ore, according to the growth curve of Stacey and Kramers (1975), regarding an estimated age between 500–600 My ago for this deposit, with a model age of 1.07 Ga (μ = 9.74).

The linearity observed by Remus *et al.* (2000) in the isotopic diagram (Fig. 7) for the sulfides of Camaquã and Santa Maria deposits establishes a correlation between the mineralizing fluids of Cu (Au-Ag) and Pb-Zn (Cu-Ag) of the Camaquã Mines, suggesting a same age for both deposits and an essentially homogeneous source. A minimal interaction with the wall rocks, however, can be admitted to explain the small scatter presented by the isotopic compositions. The subparallel adjustment of this set of isotopic data with the reference isochrone of the Acampamento Velho Formation at Camaquã Mines indicates these deposits probably formed at 565 My ago.

The isotopic data of the analyzed sulfides in this work were plotted onto the Zartman and Doe (1981) diagrams, falling on the Orogen evolution curve (Fig. 8), which suggest
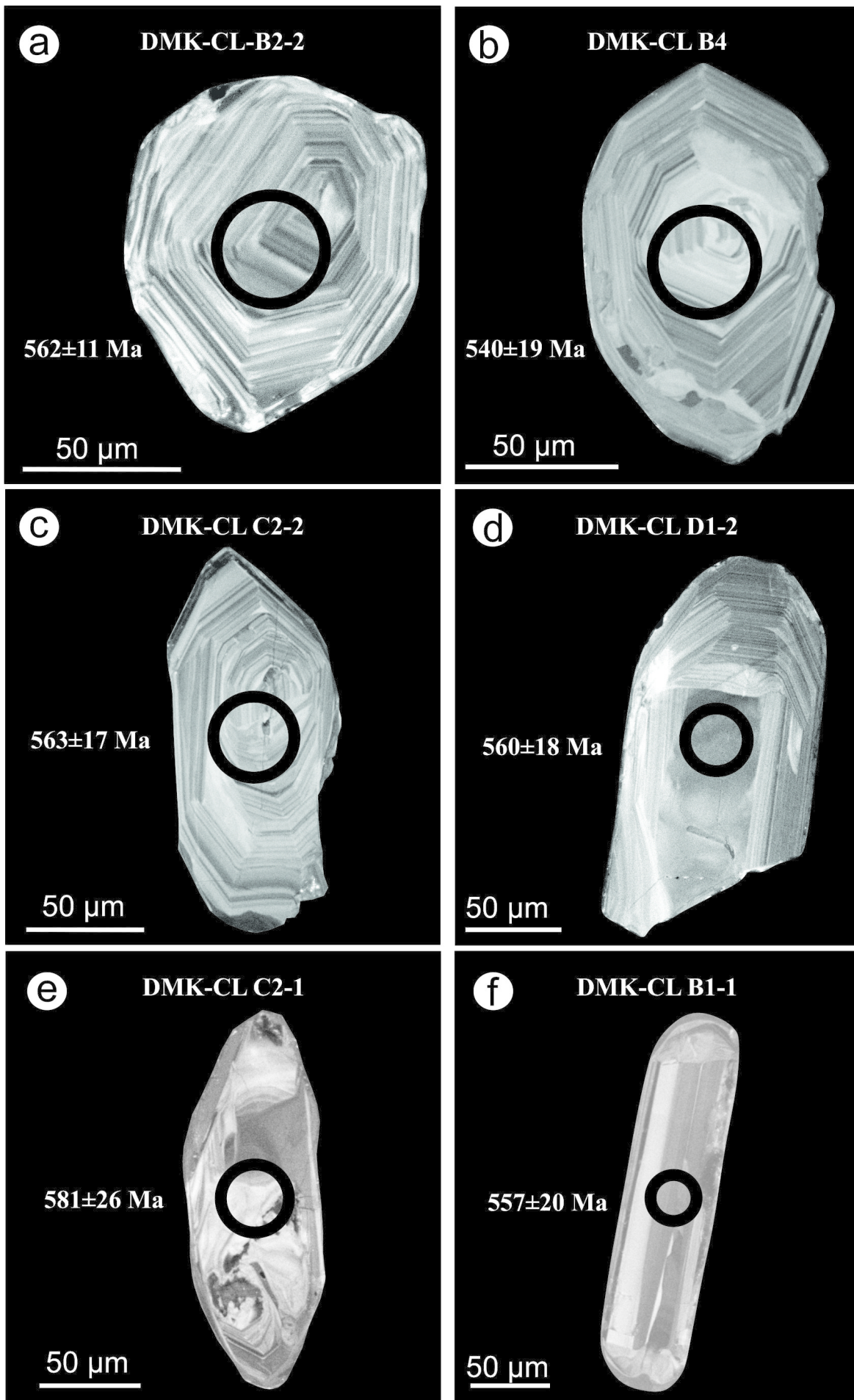
Figure 4. SEM cathodoluminescence images of magmatic zircon crystals used for DMK-CL trachyte dating, with an indication (circumference) of the position and age of the analytical points (spots); (A, B, C, and D) crystals of morphological group 1; (E and F) crystals of morphological group 2.

Table 1. U-Pb data from DMK-CL trachyte interbedded with sedimentary rocks from the Rincão dos Mouras Formation.

Zircon	f_{206}[a]	Pb ppm	Th ppm	U ppm	Th/U[b]	Isotopic Ratios[c]							Ages (Ma)						
						207Pb/235U	1 s [%]	206Pb/238U	1 s [%]	Rho[d]	207Pb/206Pb[e]	1 s [%]	206Pb/238U	1 s abs	207Pb/235U	1 s abs	207Pb/206Pb	1 s abs	% Conc[f]
From trachyte																			
DMK-CL B1-1	0.0005	14.8	216.1	162.4	1.34	0.7253	5.01	0.0902	3.59	0.72	0.0583	3.50	557	20	554	28	541	19	103
DMK-CL B2-2	0.0047	4.2	21.3	33.4	0.64	0.7446	3.45	0.0911	2.05	0.60	0.0593	2.77	562	12	565	19	576	16	98
DMK-CL B3	0.0056	4.6	38.1	36.2	1.06	0.7499	4.39	0.0921	2.30	0.52	0.0591	3.74	568	13	568	25	570	21	100
DMK-CL B4	0.0031	1.8	9.2	9.7	0.95	0.7034	5.83	0.0873	3.54	0.61	0.0584	4.63	540	19	541	32	545	25	99
DMK-CL C2-1	0.0064	15.2	76.8	105.7	0.73	0.7723	5.70	0.0942	4.44	0.78	0.0594	3.57	581	26	581	33	583	21	100
DMK-CL C2-2	0.0025	2.5	11.2	17.6	0.64	0.7456	4.91	0.0913	2.96	0.60	0.0592	3.92	563	17	566	28	576	23	98
DMK-CL C3-1	0.0063	18.2	59.8	151.3	0.40	0.7555	4.87	0.0926	3.63	0.75	0.0592	3.25	571	21	571	28	573	19	100
DMK-CL C3-2	0.0044	4.3	24.5	30.6	0.80	0.7627	3.43	0.0934	2.36	0.69	0.0592	2.49	575	14	576	20	576	14	100
DMK-CL D1-2	0.0064	2.2	14.4	16.2	0.90	0.7303	6.19	0.0906	4.04	0.65	0.0585	4.69	559	23	557	34	547	26	102
Inherited from basement or country rocks																			
DMK-CL A1-1	0.0034	28.8	186.8	563.6	0.33	0.8574	3.79	0.1010	2.21	0.58	0.0616	3.08	620	14	629	24	659	20	94
DMK-CL A1-2	0.0041	2.4	11.6	18.2	0.64	0.9343	5.04	0.1120	2.04	0.41	0.0605	4.61	684	14	670	34	621	29	110
DMK-CL A4	0.0024	4.4	21.7	29.3	0.75	0.9574	4.50	0.1096	2.72	0.60	0.0634	3.59	670	18	682	31	720	26	93
DMK-CL A6 (1)	0.0080	7.7	2.1	36.0	0.06	2.0525	4.94	0.1952	3.12	0.63	0.0763	3.83	1149	36	1133	56	1102	42	104
DMK-CL A6 (2)	0.0026	25.2	21.6	67.6	0.32	6.4671	2.75	0.3777	1.81	0.66	0.1242	2.06	2066	37	2041	56	2017	42	102
DMK-CL B5	0.0023	9.4	9.2	20.4	0.45	6.3058	1.55	0.3672	0.99	0.64	0.1245	1.20	2016	20	2019	31	2022	24	100
DMK-CL C1	0.0021	4.1	15.4	28.3	0.55	0.8926	6.03	0.1072	4.36	0.72	0.0604	4.16	657	29	648	39	617	26	106
DMK-CL C5	0.0025	2.8	24.0	15.3	1.58	1.1302	5.23	0.1248	3.74	0.71	0.0657	3.66	758	28	768	40	796	29	95
DMK-CL D1-1	0.0053	73.6	48.2	110.4	0.44	8.9645	2.03	0.4415	1.06	0.52	0.1473	1.73	2357	25	2334	47	2314	40	102
DMK-CL D2-2	0.0047	2.4	10.3	15.9	0.65	1.2690	4.76	0.1389	3.25	0.68	0.0663	3.49	838	27	832	40	815	28	103
DMK-CL E1	0.0062	15.6	37.8	134.2	0.28	0.8481	4.11	0.1010	2.43	0.59	0.0609	3.31	620	15	624	26	637	21	97
DMK-CL F1	0.0036	6.8	4.9	69.0	0.07	1.1415	4.76	0.1271	2.63	0.55	0.0651	3.97	771	20	773	37	779	31	99
Discordant																			
DMK-CL A2-1	0.0005	38.6	47.9	115.8	0.42	4.5666	1.86	0.2781	0.75	0.40	0.1191	1.70	1582	12	1743	32	1943	33	81
DMK-CL A2-2	0.0044	3.7	19.1	24.9	0.77	0.9135	5.03	0.1340	1.81	0.36	0.0494	4.69	811	15	659	33	168	8	481
DMK-CL A3	0.0020	7.1	11.6	22.0	0.53	4.6151	3.35	0.2821	2.13	0.64	0.1186	2.59	1602	34	1752	59	1936	50	83
DMK-CL B1-2	0.0013	4.4	17.1	30.1	0.57	0.8234	4.56	0.1059	2.80	0.61	0.0564	3.61	649	18	610	28	469	17	138
DMK-CL B2-1	0.0056	35.8	9.3	88.6	0.11	10.7623	3.85	0.3997	3.56	0.92	0.1953	1.48	2168	77	2503	96	2787	41	78
DMK-CL D2-1	0.0067	19.4	13.9	126.5	0.11	1.0634	3.72	0.1266	2.01	0.54	0.0609	3.13	769	15	736	27	636	20	121
DMK-CL D3	0.0067	18.4	26.3	38.4	0.69	6.3212	2.42	0.3444	2.19	0.90	0.1331	1.03	1908	42	2021	49	2139	22	89

[a]Fraction of the non-radiogenic ^{206}Pb in the analyzed zircon spot, where $f_{206} = (^{206}Pb/^{204}Pb)_c / (^{206}Pb/^{204}Pb)_s$ (c = common; s = sample); [b]Th/U ratios and amount of Pb, Th, and U (in ppm) are calculated relative to the GJ-1 reference zircon; [c]corrected for the analytical "blanc" (background) and Pb/U internal fractionation, and normalized to GJ-1 reference zircon (ID-TIMS-values/measured values); ^{207}Pb/^{235}U calculated through the equation = $(^{207}Pb/^{206}Pb)*(^{206}Pb/^{238}U)*(137,88)$; [d]Rho is the error correlation defined as the quotient of the propagated errors ^{206}Pb/^{238}U and ^{207}Pb/^{235}U ratios; [e]corrected for mass-bias by normalization to GJ-1 reference zircon and common Pb using the model of Stacey and Kramers (1975); [f]degree of concordance = $(^{206}Pb/^{238}U \text{ age} \times 100) / (^{207}Pb/^{206}Pb \text{ age})$.
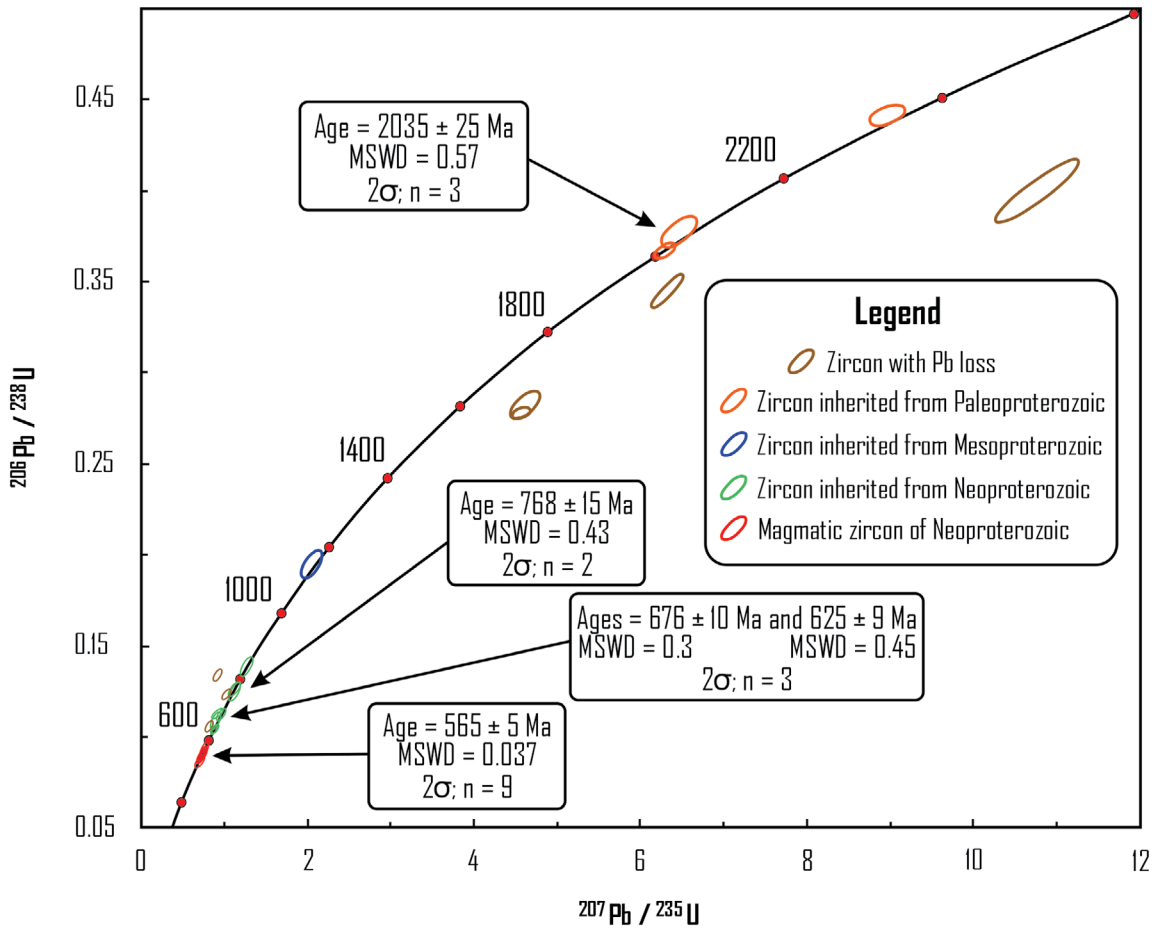
Figure 5. Concordia diagram for all the zircon populations from the DMK-CL trachyte interbedded with the rocks of the Rincão dos Mouras Formation.
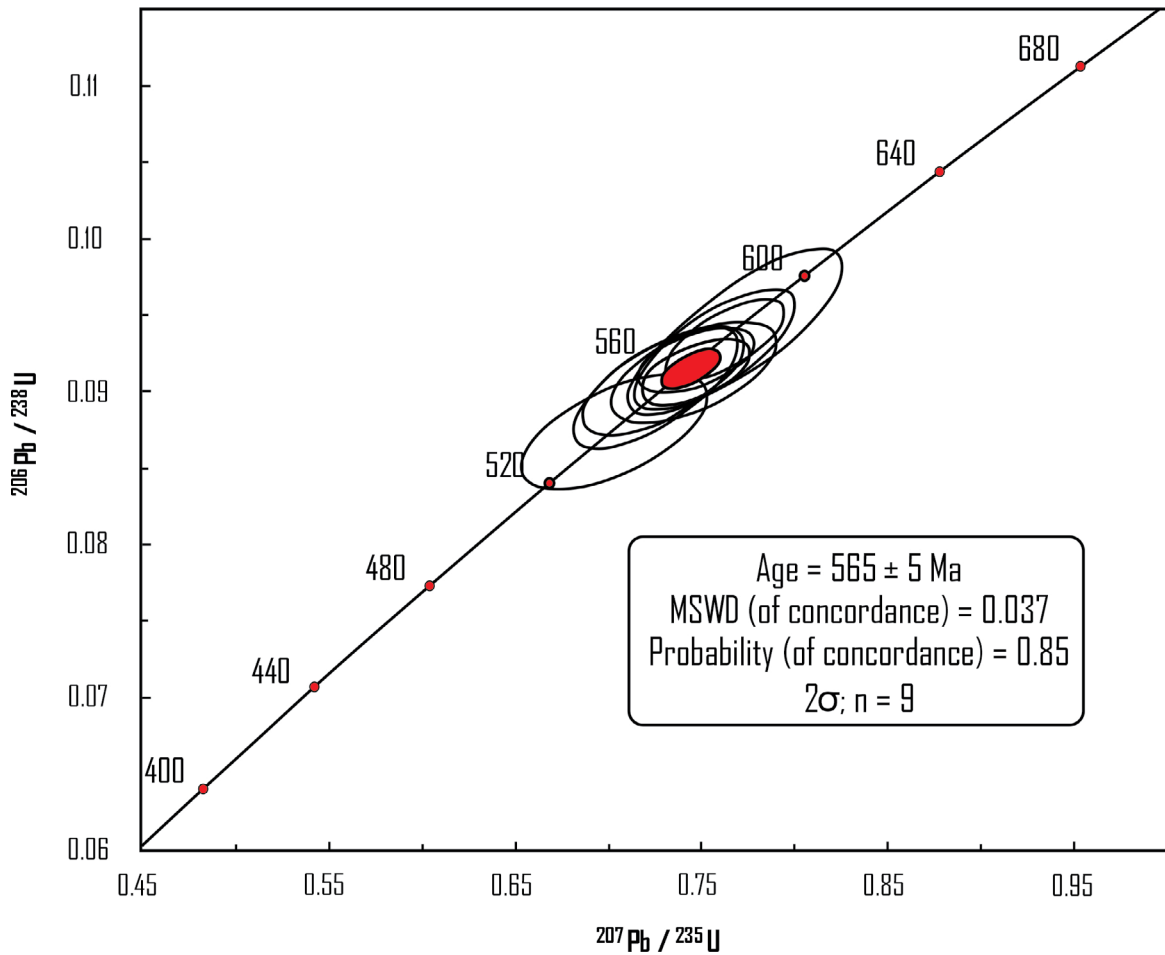

Figure 6. Concordia diagram for the youngest Neoproterozoic zircon population from the trachyte DMK-CL sample from Camaquã Mines region.

Table 2. Ages obtained for the Acampamento Velho Formation in different localities of the Camaquã Basin.

Locality	Rock	Age (Ma)	Method	Reference
Camaquã Basin	Rhyolite	545 ± 13	Rb-Sr	Almeida *et al.* (1996)
Perau Hill	Rhyolite	573 ± 18	U-Pb SHRIMP	Chemale Jr. (2000)
Martins Hill	Qtz-diorite	550 ± 5	Pb-Pb evaporation	Toniolo *et al.* (2004)
Ramada Plateau	Subvolcanic rhyolite	549 ± 5	U-Pb SHRIMP	Sommer *et al.* (2005)
Ramada Plateau	Rhyolite	574 ± 7	U-Pb TIMS	Janikian *et al.* (2008)
Bugio Hill	Basalt	553 ± 5	U-Pb LA-ICP-MS	Almeida *et al.* (2012)
Taquarembó Plateau	Acid tuff	553 ± 17	U-Pb LA-ICP-MS	Janikian *et al.* (2012)
Bom Jardim	Subvolcanic rhyolite	572 ± 7	U-Pb LA-ICP-MS	Janikian *et al.* (2012)
Ramada Plateau	Subvolcanic rhyolite	562 ± 2	U-Pb LA-ICP-MS	Matté *et al.* (2016)
Ramada Plateau	Rhyolitic ignimbrite	560 ± 2	U-Pb LA-ICP-MS	Matté *et al.* (2016)
Ramada Plateau	Rhyolitic ignimbrite	561 ± 2	U-Pb LA-ICP-MS	Matté *et al.* (2016)
Ramada Plateau	Subvolcanic trachyte	560 ± 14	U-Pb LA-ICP-MS	Matté *et al.* (2016)
Tupanci Hill	Rhyolite	579 ± 6	U-Pb LA-ICP-MS	Sommer *et al.* (2017)
Picados Hill	Rhyolite	558 ± 39	U-Pb LA-ICP-MS	Sommer *et al.* (2017)
Palma	Basalt	572 ± 6	U-Pb LA-ICP-MS	Vedana *et al.* (2017)
Palma	Andesitic basalt	563 ± 2	U-Pb LA-ICP-MS	Vedana *et al.* (2017)
Camaquã Mines	**Trachyte**	**565 ± 5**	**U-Pb LA-ICP-MS**	**This work**
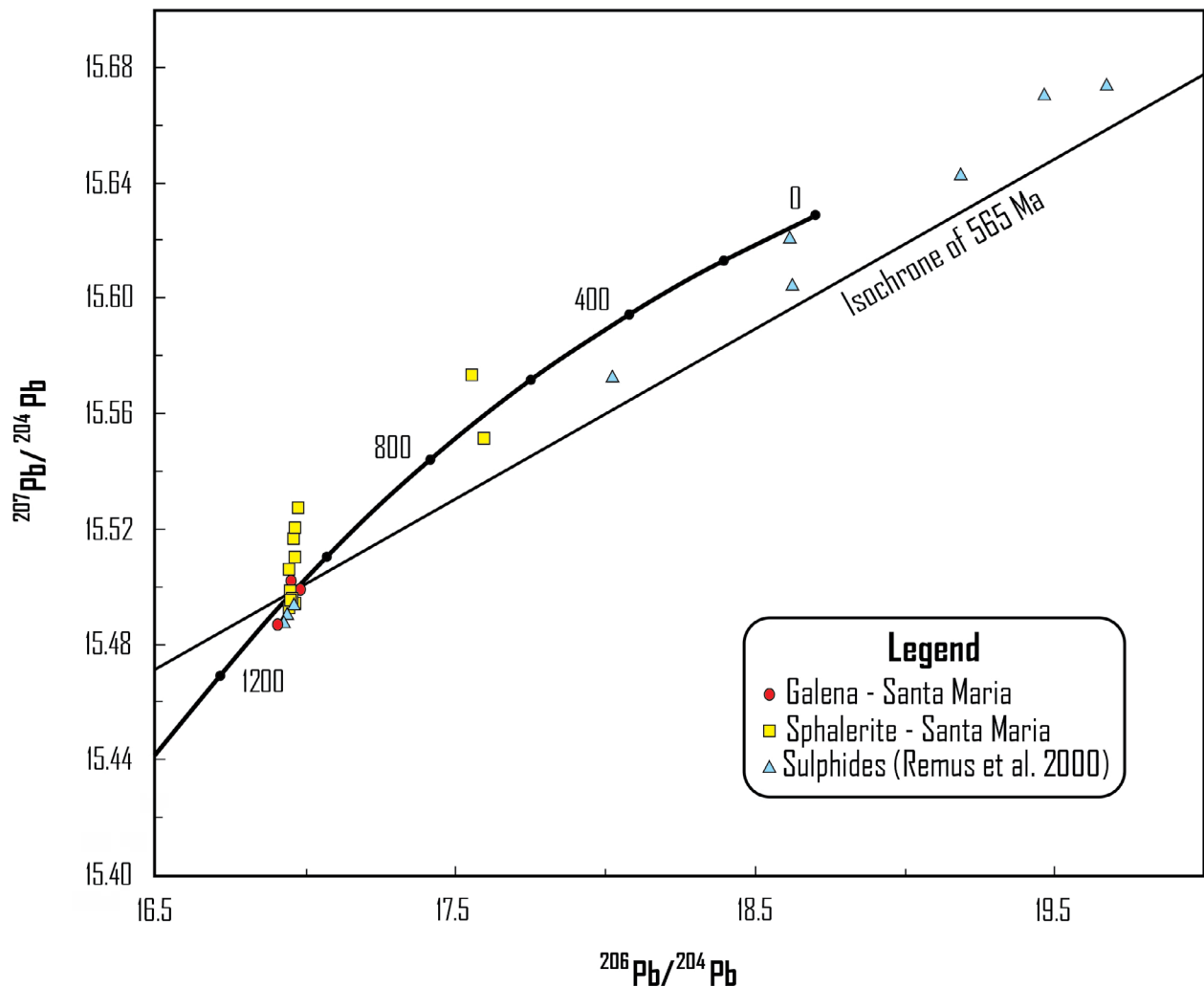
Figure 7. Pb-Pb diagram presenting sulfide (galena and sphalerite) isotopic data from the Santa Maria deposit obtained in this work. Data from Remus *et al.* (2000), the 565 Ma reference isochrone for Acampamento Velho magmatism at the Camaquã Mines (this work), and the growth curve of Stacey and Kramers (1975) are also plotted for comparison.

an intermediate or mixed origin for the Pb of the Santa Maria deposit and indicate a model age of 1.1 to 1.2 Ga. In the thorogenic diagram (Fig. 9), the data plot between Mantle, Orogen and Lower Crust curves, being mostly nearer to the latter, which points out to a high Th/U source contribution. It is also possible to observe that only the ^{206}Pb/^{204}Pb isotopic ratios had a significant variation, highlighting the homogeneity of the ^{208}Pb/^{204}Pb ratios, as well as the consistency between the present isotopic data and those from Remus *et al.* (2000) for galena and sphalerite.

DISCUSSION AND CONCLUSIONS

The age of 565 ± 5 Ma obtained for the trachytic DMK-CL sample allowed us to identify, in an unprecedented way, the occurrence of the Acampamento Velho Formation in the region of the Camaquã Mines.

The two trachytic rocks (one in PCSM79-14 drill hole, at Area 1, and the other in FSM 81 drill hole, at Claudino Farm) have similar mineral composition and both present evidence of contemporary genesis with the sedimentary country rocks. The peperitic features found on the mineralized subvolcanic trachyte sill upper contact, at Area 1 of the Santa Maria deposit, indicate magma-wet sediment interaction. The age obtained for the DMK-CL sample (565 ± 5 Ma), located at the Claudino farm, is equivalent to the maximum depositional age of the Santa Barbara Group (566 ± 7 Ma; Bicca *et al.* 2013; 568 ± 6 Ma; Oliveira *et al.* 2014), determined from the dating of detrital zircon crystals. This is probably due to the fact that trachyte intruded wet sediments as a subvolcanic sill, like Area 1 trachytic rock, or means it is formed as a lava flow during a rapid succession of sedimentation and magmatic events. The concordant character of this rock with its wall rocks is in agreement with both hypotheses.

From this contemporaneity relationship, it is possible to infer an approximate age for the Area 1 trachyte sill rock. Such rock occurs in a lower stratigraphic level (Seival Formation) relatively to Claudino farm rock (Rincão dos Mouras Formation). Thus, its age should necessarily be between DMK-CL sample age and the maximum depositional age of the Santa Barbara Group. As these ages are equivalent, Area 1 trachyte sill has approximately the same age as the Claudino farm trachyte. Therefore, the Acampamento Velho magmatism in the region of the Camaquã Mines is represented by both rocks.

The fact that galena and sphalerite have, in essence, the same Pb isotopic composition suggests a homogeneous source for

Table 3. Pb isotopic ratios obtained for the sulfides from the Santa Maria deposit. Similar data from Remus *et al.* (2000) are also presented, for which the total analytical error for each Pb isotopic ratio corresponds to ± 0.15%.

Sample	Mineral	^{206}Pb/^{204}Pb	2s	^{207}Pb/^{204}Pb	2s	^{208}Pb/^{204}Pb	2s
A1-10	GALENA	16.950	0.001	15.502	0.001	37.619	0.002
A2-5	GALENA	16.905	0.002	15.487	0.002	37.577	0.004
A3-5	GALENA	16.983	0.001	15.499	0.001	37.591	0.002
A3-7 L1	SPHALERITE	16.965	0.002	15.521	0.002	37.659	0.005
A3-7 L2	SPHALERITE	16.963	0.004	15.511	0.004	37.632	0.010
A3-7 L3	SPHALERITE	16.947	0.002	15.499	0.002	37.601	0.005
A3-7 L4	SPHALERITE	16.973	0.003	15.528	0.003	37.688	0.007
A3-7 L5	SPHALERITE	16.956	0.001	15.497	0.001	37.598	0.003
A3-7 L6	SPHALERITE	17.595	0.002	15.552	0.002	37.627	0.004
A3-8 L1	SPHALERITE	16.945	0.002	15.507	0.002	37.628	0.005
A3-8 L2	SPHALERITE	16.947	0.002	15.496	0.002	37.581	0.004
A3-8 L3	SPHALERITE	16.945	0.001	15.493	0.001	37.572	0.002
A3-8 L4	SPHALERITE	16.960	0.001	15.517	0.001	37.652	0.002
A3-8 L5	SPHALERITE	16.963	0.001	15.495	0.001	37.582	0.002
A3-8 L6	SPHALERITE	17.555	0.011	15.574	0.010	37.737	0.025
Data from Remus *et al.* (2000)							
MSMA-G	GALENA	16.927	-	15.488	-	37.559	-
MSMC-G	GALENA	16.950	-	15.502	-	37.625	-
MSB-B gn	GALENA	16.960	-	15.494	-	37.550	-
MSMC-S	SPHALERITE	16.939	-	15.491	-	37.576	-
CB-199E.P20	CHALCOPYRITE I	19.468	-	15.671	-	40.320	-
CB-199E.P20	PYRITE	19.185	-	15.643	-	39.476	-
CB.P-19	PYRITE	18.626	-	15.605	-	38.933	-
CB.P-19	CHALCOPYRITE	18.616	-	15.621	-	39.064	-
CB-282A	CHALCOPYRITE	18.024	-	15.573	-	38.208	-
TV-211	PIR/CALCOP II	19.672	-	15.674	-	39.438	-

the several ore bodies in the Santa Maria deposit. The small scatter these sulfides present can result of a minimal contamination of the ore fluid by the wall rocks. The isotopic data of ore samples from the Camaquã (Cu; Au-Ag) and Santa Maria (Pb-Zn; Cu-Ag) deposits form a linear trend. While this trend does not correspond to a true isochron, possibly due to the contribution of old radiogenic Pb derived from U-Th-rich inclusions within ore pyrites (Remus *et al.* 2000), it suggests a simultaneous genesis and, again, an essentially homogeneous isotopic system for the Camaquã Mines deposits.
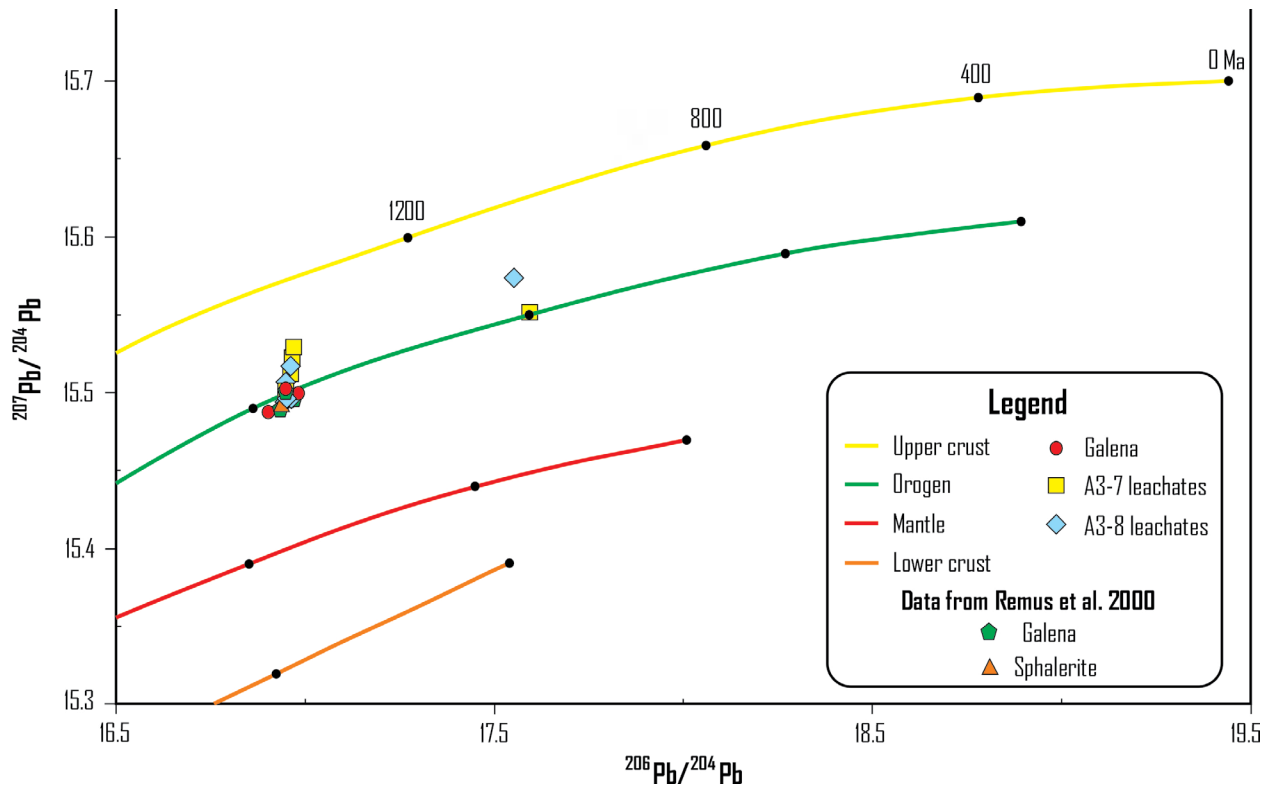
Figure 8. Galena and sphalerite isotopic data obtained in this study plotted on the 207Pb/206Pb diagram (Zartman and Doe 1981), indicating an orogenic or mixed origin for the Santa Maria mineralization, and a 1.1 to 1.2 Ga model age. Data from Remus *et al.* (2000) for the same sulfides are shown for comparison.
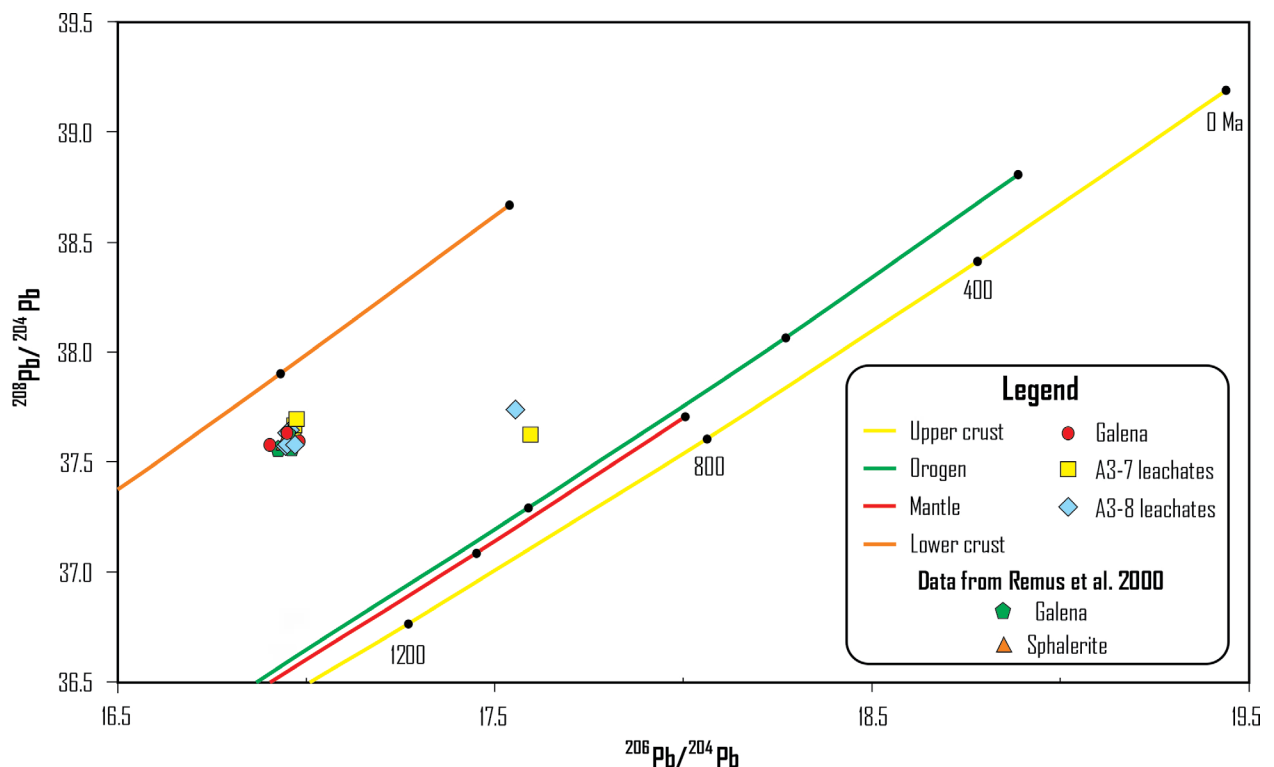
Figure 9. Galena and sphalerite isotopic data obtained in this study plotted on the 208Pb/206Pb diagram (Zartman and Doe 1981), demonstrating homogeneity of the 208Pb/204Pb ratios and indicating a thorogenic contribution. Data from Remus *et al.* (2000) for the same sulfides are shown for comparison.

Remus *et al.* (2011) studied Crespos Cu-sulphide ore deposit, hosted by Acampamento Velho Formation rhyolites, and observed the Pb isotopic composition of this mineralization is similar to the least radiogenic compositions of Santa Maria, Camaquã, and Cerro dos Martins deposits. Based on these and other data, the authors did conclude these deposits are genetically related to the Acampamento Velho Formation magmatism, developed about 545 ± 13 Ma (Rb-Sr; Almeida *et al.* 1996).

These authors' conclusion was reinforced in this work by the spatial association observed in the field between trachytic rocks and mineralization, both related to the same hydrothermal process, as well as by the genetic association between this alkaline magmatism and mineralization pointed out by the subparallel nature between the linear arrangement formed by the Pb isotopic compositions of the Camaquã and Santa Maria sulfides and the reference isochrone of 565 Ma for the Acampamento Velho Formation (this work). However, as the isochrone inclination is not sensible enough to distinguish possible different ages to these ore deposits, Acampamento Velho Formation is seen here as only a possible magmatic candidate to be genetically associated to these deposits. Further studies are necessary to elucidate this topic.

Isotopic data also suggest a dominantly crustal and ancient basement source for Pb, with a model age of 1.07 Ga. Although rocks of such an age are unknown in the Camaquã Basin and its basement, they possibly occur at greater depths. Similar ages were obtained in inherited detrital zircon crystals (1.2 to 1.0 Ga) in the Sul-Riograndense Shield, whose source has not yet been identified (Remus *et al.* 1999, Hartmann *et al.* 2016). An igneous/metamorphic old rock with galena was probably the lead source for the Camaquã and Santa Maria deposits.

Galena and sphalerite Pb isotopic ratios of the Santa Maria deposit fall along the Orogen curve of Zartman and Doe (1981), which indicates an intermediate or mixed origin for these sulfides. These data also plot between Mantle, Orogen, and Lower Crust curves, being mostly nearer to the latter, in the thorogenic diagram. This points out to a lower crust contribution to the ore source rock magma.

From the data presented so far, it's possible to conclude that magmatic-hydrothermal fluids, possibly from the Acampamento Velho magmatism at the Camaquã Mines region, leached metals from an igneous or metamorphic deep old rock, with little wall rock interaction during its ascendant movement. Another valid hypothesis is that this ancient rock not only provided the metals, but also gave origin, by partial melting, to the parental magma of the trachytic rocks. In one way or another, the isotopic homogeneity observed in the sulfides is explained.

ACKNOWLEDGMENTS

REFERENCES

Allen R.L. 1992. Reconstruction of the tectonic, volcanic and sedimentary setting of strongly deformed Zn-Cu massive sulfide deposits at Benambra, Victoria. *Economic Geology*, **87**(3):825-854. https://doi.org/10.2113/gsecongeo.87.3.825

Almeida D.P.M., Chemale Jr. F., Machado A. 2012. Late to Post-Orogenic Brasiliano-Pan-African Volcano-Sedimentary Basins in the Dom Feliciano Belt, Southernmost Brazil. *In*: Al-Juboury A.I. (Ed.). *Petrology: New Perspectives and Applications*. Rijeka: InTech, v. 1, p. 73-130. https://doi.org/10.5772/25189

Almeida D.P.M., Zerfass H., Basei, M.A. 1996. Mineralogia, geoquímica e novas idades para o vulcanismo ácido da Bacia do Camaquã. *In*: Congresso Brasileiro de Geologia, 39., 1996, Salvador. *Annals...*, v. 2, p. 19-21.

Almeida D.P.M., Zerfass H., Basei M.A., Petry K., Gomes C.H. 2002. The Acampamento Velho Formation, a Lower Cambrian bimodal volcanic package: geochemical and stratigraphic studies from the Cerro do Bugio, Perau and Serra de Santa Bárbara (Caçapava do Sul, Rio Grande do Sul, RS. Brazil). *Gondwana Research*, **5**(3):721-733. https://doi.org/10.1016/S1342-937X(05)70640-7

Almeida R.P. 2005. *Tectônica e sedimentação do Ediacarano ao Ordoviciano: exemplos do Supergrupo Camaquã (RS) e do Grupo Caacupé (Paraguai Oriental)*. PhD Thesis, Universidade de São Paulo, São Paulo, 216p.

Babinski M., Chemale Jr. F., Hartmann L.A., Van Schmus W.R., Silva L.C. 1996. Juvenile accretion at 750–700 Ma in southern Brazil. *Geology*, **24**(5):439-442. https://doi.org/10.1130/0091-7613(1996)024%3C0439:JAAMIS%3E2.3.CO;2

Badi W.S.R. 1987. *Relatório final de pesquisa*. Porto Alegre: CBC, 120p.

Badi W.S.R., Gonzalez A.P. 1988. Jazida de metais básicos de Santa Maria, Caçapava do Sul, Rio Grande do Sul. *In*: Schobbenhaus C., Coelho C.E.S. (Eds). *Principais Depósitos Minerais do Brasil*. Brasil: DNPM-CVRD, p. 157-170.

Beckel J. 1992. Características físico-químicas do fluido hidrotermal formador das mineralizações de cobre das minas do Camaquã, RS. *In*: Workshop sobre as Bacias Molássicas Brasilianas, São Leopoldo. *Boletim de Resumos Expandidos*, v. 1, p. 6-11.

Bettencourt J.S. 1972. *A mina de cobre de Camaquã, Rio Grande do Sul*. PhD Thesis, Universidade de São Paulo, São Paulo, 196p.

Bicca M.M., Chemale Jr. F., Jelinek A.R., de Oliveira C.H.E., Guadagnin F., Armstrong R. 2013. Tectonic evolution and provenance of the Santa Bárbara Group, Camaquã Mines region, Rio Grande do Sul, Brazil. *Journal of South American Earth Sciences*, **48**:173-192. https://doi.org/10.1016/j.jsames.2013.09.006

Bitencourt M.D.F., Nardi L.V.S. 2000. Tectonic setting and sources of magmatism related to the Southern Brazilian Shear Belt. *Revista Brasileira de Geociências*, **30**(1):186-189. https://doi.org/10.25249/0375-7536.2000301186189

Borba, A.W., Mizusaki, A.M.P., Silva, D.R.A., Koester, E., Noronha, F.L., Casagrande, J. 2006. Provenance of the Neoproterozoic Maricá Formation (Sul-rio-grandense Shield, southern Brazil): petrographic and Sm-Nd isotopic constraints. *Gondwana Research*, **9**(4), 464-474. https://doi.org/10.1016/j.gr.2006.01.005

Brito Neves B.B., Cordani U.G. 1991. Tectonic evolution of South America during the late Proterozoic. *Precambrian Research*, **53**(1-2):23-40. https://doi.org/10.1016/0301-9268(91)90004-T

Busby-Spera C.J., White J.D. 1987. Variation in peperite textures associated with differing host-sediment properties. *Bulletin of Volcanology*, **49**:765-776. https://doi.org/10.1007/BF01079827

Chemale Jr. F. 2000. Evolução geológica do Escudo Sul-rio-grandense. *In*: Holz M., De Ros L.F. (Eds.). *Geologia do Rio Grande do Sul*. Porto Alegre: CIGO/UFRGS, p. 13-52.

Corfu F., Hanchar J.M., Hoskin P.W.O., Kinny P. 2003. Atlas of zircon textures. *Reviews in Mineralogy and Geochemistry*, **53**(1):469-500. https://doi.org/10.2113/0530469

De Ros, L.F.; Morad, S.; Paim, P.S.G. 1994. The role of detrital composition and climate on the diagenetic evolution of continental molasses: evidence from the Cambro-Ordovician Guaritas Sequence, southern Brazil. *Sedimentary Geology*, **92**(3-4):197-228. https://doi.org/10.1016/0037-0738(94)90106-6

Fambrini G.L. 2003. *O Grupo Santa Bárbara (Neoproterozóico III) da Bacia do Camaquã, Rio Grande do Sul*. PhD Thesis, Universidade de São Paulo, São Paulo, 243p.

Fambrini G.L., Janikian L., Paes de Almeida R., Fragoso-César A.R.S. 2005. O Grupo Santa Bárbara (Ediacarano) na sub-bacia Camaquã Central, RS: estratigrafia e sistemas deposicionais. *Revista Brasileira de Geociências*, **35**(2):227-238.

Fernandes L.A.D., Tommasi A., Porcher C.C. 1992. Deformation patterns in the southern Brazilian branch of the Dom Feliciano Belt: a reappraisal. *Journal of South American Earth Sciences*, **5**(1):77-96. https://doi.org/10.1016/0895-9811(92)90061-3

Fragoso-Cesar A.R.S., Fambrini G.L., de Almeida R.P., Pelosi A.P.M.R., Janikian L., Riccomini C., Saes G.S. 2000. The Camaquã extensional basin: Neoproterozoic to early Cambrian sequences in southernmost Brazil. *Brazilian Journal of Geology*, **30**(3):439-441. https://doi.org/10.25249/0375-7536.2000303442445

Fragoso-Cesar A.R.S., Fambrini G.L., Paes de Almeida R., Pelosi A.P.M.R., Janikian L. 2003. A Bacia Camaquã: um sistema intracontinental anorogênico de rifts do Neoproterozóico III-Eopaleozóico no Rio Grande do Sul. *In*: Encontro sobre a Estratigrafia do Rio Grande do Sul: Escudos e Bacias, 1., Porto Alegre. *Boletim de Resumos…*, p. 139-144.

Galarza M.A., Macambira M.J.B. 2002. Geocronologia e evolução crustal da área do depósito de Cu-Au Gameleira, Província Mineral de Carajás (Pará), Brasil. *Geologia USP. Série Científica*, **2**:143-159. https://doi.org/10.13140/RG.2.1.2318.3767

Gresse P.G., Chemale F., Silva L.C., Walraven F., Hartmann L.A. 1996. Late-to post-orogenic basins of the Pan-African-Brasiliano collision orogen in southern Africa and southern Brazil. *Basin Research*, **8**(2):157-171. https://doi.org/10.1046/j.1365-2117.1996.01504.x

Hartmann L.A., Lopes W.R., Savian J.F. 2016. Integrated evaluation of the geology, aerogammaspectrometry and aeromagnetometry of the Sul-Riograndense Shield, southernmost Brazil. *Anais da Academia Brasileira de Ciências*, **88**(1):75-92. https://doi.org/10.1590/0001-3765201520140495

Janikian L., Almeida R.P., Fragoso-Cesar A.R.S., Fambrini G.L. 2003. Redefinição do Grupo Bom Jardim (Neoproterozóico III) em sua área-tipo: litoestratigrafia, evolução paleoambiental e contexto tectônico. *Revista Brasileira de Geociências*, **33**(4):347-360.

Janikian L., Almeida R.P., Fragoso-Cesar A.R.S., Souza Martins V.T., Dantas E.L., Tohver E., McReath I., D'Agrella-Filho M.S. 2012. Ages (U–Pb SHRIMP and LA ICPMS) and stratigraphic evolution of the Neoproterozoic volcano-sedimentary successions from the extensional Camaquã Basin, Southern Brazil. *Gondwana Research*, **21**(2-3):466-482. https://doi.org/10.1016/j.gr.2011.04.010

Janikian L., Almeida R.P., Trindade D., Ferreira R.I., Fragoso-Cesar A.R.S., D'Agrella-Filho M.S., Dantas E.L., Tohver E. 2008. The continental record of Ediacaran volcano-sedimentary successions in southern Brazil and their global implications. *Terra Nova*, **20**(4):259-266. https://doi.org/10.1111/j.1365-3121.2008.00814.x

Laux J.H., Lindenmayer Z.G. 2000. As Minas do Camaquã: um século de evolução de hipóteses genéticas. *In*: Ronchi L.H., Lobato A.O.C. (Eds.), *Minas do Camaquã: um estudo multidisciplinar*. São Leopoldo: UNISINOS/FAPERGS, p. 133-164.

Laux J.H., Lindenmayer Z.G., Teixeira J.B.G., Bastos Neto A. 2005. Ore genesis at the Camaquã copper mine, a neoproterozoic sediment-hosted deposit in Southern Brazil. *Ore Geology Reviews*, **26**(1-2):71-89. https://doi.org/10.1016/j.oregeorev.2004.11.001

Licht O. 1980. A descoberta da Jazida Santa Maria (Zn, Pb, Cu) Rio Grande Do Sul-Brasil: um caso histórico de prospecção geoquímica. *In*: Congresso Brasileiro de Geologia, 31., Camboriú. *Anais…*, v. 1, p. 141-153.

Ludwig K. 2008. *Isoplot 3.6*. Berkeley: Berkeley Geochronology Center Special Publication, **4**, 77 p.

Manhès G. 1982. *Développement de I'ensemble chronométrique U-Th-Pb. Contribution à la chronologieinitiale du systèmesolaire*. PhD Thesis, Universidade de Paris, Paris, 249 p.

Martin U., Németh K. 2007. Blocky versus fluidal peperite textures developed in volcanic conduits, vents and crater lakes of phreatomagmatic volcanoes in Mio/Pliocene volcanic fields of Western Hungary. *Journal of Volcanology and Geothermal Research*, **159**(1-3):164-178. https://doi.org/10.1016/j.jvolgeores.2006.06.010

Matté V., Sommer C.A., de Lima E.F., Philipp R.P., Basei M.A.S. 2016. Post-collisional Ediacaran volcanism in oriental Ramada Plateau, southern Brazil. *Journal of South American Earth Sciences*, **71**:201-222. https://doi.org/10.1016/j.jsames.2016.07.015

Milhomem Neto J.M., Lafon J.M. 2019. Zircon U-Pb and Lu-Hf isotope constraints on Archean crustal evolution in Southeastern Guyana Shield. *Geoscience Frontiers*, **10**(4):1477-1506. https://doi.org/10.1016/j.gsf.2018.09.012

Nardi L.V.S., Lima E.D. 1985. A associação shoshonítica de Lavras do Sul, RS. *Revista Brasileira de Geociências*, **15**(2):139-146.

Oliveira C.H.E., Chemale Jr. F., Jelinek A.R., Bicca M.M., Philipp R.P. 2014. U–Pb and Lu–Hf isotopes applied to the evolution of the late to post-orogenic transtensional basins of the Dom Feliciano belt, Brazil. *Precambrian Research*, **246**:240-255. https://doi.org/10.1016/j.precamres.2014.03.008

Paim P.S.G., Chemale Jr. F., Lopes R.C. 2000. A Bacia do Camaquã. *In*: Holz M., De Ros L.F. (Eds.). *Geologia do Rio Grande do Sul*. Porto Alegre: CIGO/UFRGS, p. 231-274.

Remus M.V.D., Hartmann L.A., McNaughton N.J., Groves D.I., Reischl J.L. 2000. A distal magmatic-hydrothermal origin for the Camaquã Cu (Au-Ag) and Santa Maria Pb-Zn (Cu-Ag) deposits, southern Brazil. *Gondwana Research*, **3**(2):155-174. https://doi.org/10.1016/S1342-937X(05)70094-0

Remus M.V., Hartmann L.A., Toniolo J.A. 2011. Low-temperature, hydrothermal base and precious metal deposits hosted by volcanic-sedimentary sequences of the Camaquã basin, southernmost Brazil. *In*: European Geosciences Union General Assembly, Vienna. *Poster*.

Remus M.V.D., McNaughton N.J., Hartmann L.A., Koppe J.C., Fletcher I.R., Groves D.I., Pinto V.M. 1999. Gold in the Neoproterozoic juvenile Bossoroca Volcanic Arc of southernmost Brazil: isotopic constraints on timing and sources. *Journal of South American Earth Sciences*, **12**(4):349-366. https://doi.org/10.1016/S0895-9811(99)00026-7

Renac C., Mexias A.S., Gomes M.E.B., Ronchi L.H., Nardi L.V.S., Laux J.H. 2014. Isotopic fluid changes in a Neoproterozoic porphyry–epithermal system: The Uruguay mine, southern Brazil. *Ore Geology Reviews*, **60**:146-160. http://doi.org/10.1016/j.oregeorev.2013.12.016

Ribeiro M., Bocchi P.R., Figueiredo F.P.M., Tessari R.I. 1966. *Geologia da quadrícula de Caçapava do Sul, RS, Brasil*. Rio de Janeiro: DNPM/DFPM, 232p. (Bulletin 127).

Ronchi L.H., Lindenmayer Z.G., Bastos Neto A., Murta C.R. 2000. O stockwork e a zona do minério sulfetado no arenito inferior da Mina Uruguai, RS. *In*: Ronchi L.H., Lobato A.O.C. (Eds.). *Minas do Camaquã:* um estudo multidisciplinar. São Leopoldo: UNISINOS/FAPERGS, p. 165-190.

Skilling I.P., White J.D.L., McPhie J. 2002. Peperite: a review of magma–sediment mingling. *Journal of Volcanology and Geothermal Research*, **114**(1-2):1-17. https://doi.org/10.1016/S0377-0273(01)00278-5

Sommer C.A., Leitzke F.P., Lima E.F.D., Barreto C.J.S., Lafon J.M., Matté V., Philipp R.P., Conceição R.V., Basei M.Â.S. 2017. Zircon U-Pb geochronology, Sm-Nd and Pb-Pb isotope systematics of Ediacaran post-collisional high-silica Acampamento Velho volcanism at the Tupanci area, NW of the Sul-Rio-Grandense Shield, Brazil. *Brazilian Journal of Geology*, **47**(4):545-560. https://doi.org/10.1590/2317-4889201720170064

Sommer C.A., Lima E.F., Nardi L.V.S., Figueiredo A.M.G., Pierosan R. 2005. Potassic and low- and high-Ti mildly alkaline volcanism in the Neoproterozoic Ramada Plateau, southernmost Brazil. *Journal of South American Earth Sciences*, **18**(3-4):237-254. https://doi.org/10.1016/j.jsames.2004.11.003

Stacey J.S., Kramers J.D. 1975. Approximation of terrestrial lead isotope evolution by a two-stage model. *Earth and Planetary Science Letters*, **26**(2):207-221. https://doi.org/10.1016/0012-821X(75)90088-6

Teixeira G., Gonzalez A.P. 1988. Minas do Camaquã, Município de Caçapava do Sul, RS. *In*: Schobbenhaus C., Coelho C.E.S. (Eds). *Principais Depósitos Minerais do Brasil*. Brasil: DNPM-CVRD, p. 33-41.

Teixeira G., Gonzalez A.P., Gonzalez M.A., Licht O.A.B. 1978. Situação das Minas do Camaquã, Rio Grande do Sul. *In*: Congresso Brasileiro de Geologia, 30., Recife. *Anais…*, v. 6, p. 1893-1905.

Toniolo J.A., Remus M.V.D., Macambira M.J.B., Moura C.A.V. 2004. Metalogênese do Depósito de Cobre Cerro dos Martins, RS, Revisão e Geoquímica Isotópica de Sr, S, O e C. *Pesquisas em Geociências*, **31**(2):41-67. https://doi.org/10.22456/1807-9806.19573

Vedana L.A., Philipp R.P., Sommer C.A. 2017. Post-collisional basalts of the Acampamento Velho Formation, Camaquã Basin, São Gabriel Terrane, southernmost Brazil. *Brazilian Journal of Geology*, **47**(3):467-489. https://doi.org/10.1590/2317-4889201720170019

Xiang W., Griffin W.L., Jie C., Pinyun H., Xiang L.I. 2011. U and Th contents and Th/U ratios of zircon in felsic and mafic magmatic rocks: Improved zircon-melt distribution coefficients. *Acta Geologica Sinica*, **85**(1):164-174. https://doi.org/10.1111/j.1755-6724.2011.00387.x

Wildner W., Lima E.F., Nardi L.V.S., Sommer C.A. 2002. Volcanic cycles and setting in the Neoproterozoic III to Ordovician Camaquã Basin succession in southern Brazil: characteristics of post-collisional magmatism. *Journal of Volcanology and Geothermal Research*, **118**(1-2):261-283. https://doi.org/10.1016/S0377-0273(02)00259-7

Zartman R.E., Doe B.R. 1981. Plumbotectonics - the model. *Tectonophysics*, **75**(1-2):135-162. https://doi.org/10.1016/0040-1951(81)90213-4